Journal of Applied Physics

# Persistent phosphors for the future: Fit for the right application

Cite as: J. Appl. Phys. **128**, 240903 (2020); https://doi.org/10.1063/5.0032972
Submitted: 12 October 2020 . Accepted: 14 November 2020 . Published Online: 24 December 2020

Dirk Poelman, David Van der Heggen, Jiaren Du, Ewoud Cosaert, and Philippe F. Smet

Journal of Applied Physics PERSPECTIVE scitation.org/journal/jap

# Persistent phosphors for the future: Fit for the right application

Cite as: J. Appl. Phys. **128**, 240903 (2020); doi: 10.1063/5.0032972
Submitted: 12 October 2020 · Accepted: 14 November 2020 ·
Published Online: 24 December 2020



Dirk Poelman,[a] David Van der Heggen, Jiaren Du, Ewoud Cosaert, and Philippe F. Smet

## AFFILIATIONS

LumiLab, Department of Solid State Sciences, Ghent University, Krijgslaan 281-S1 B-9000, Ghent, Belgium

[a]**Author to whom correspondence should be addressed:** dirk.poelman@ugent.be

## ABSTRACT

When the bright green-emitting $SrAl_2O_4$:Eu,Dy persistent phosphor was described in the literature in 1996, this presented a real breakthrough in performance, both in terms of initial brightness and afterglow duration. Since then, many new persistent phosphors, with emission spanning from the ultraviolet to the near infrared, have been developed. Very few materials, however, reach a similar afterglow time and intensity as $SrAl_2O_4$:Eu,Dy, which is still considered the benchmark phosphor. The present paper discusses the reasons for this—seemingly—fundamental limitation and gives directions for further improvements. An overview is given of the preparation methods of persistent phosphors and their properties. Much attention is paid to the correct evaluation of a persistent phosphor in absolute units rather than vague terms or definitions. State of the art persistent phosphors are currently used extensively in emergency signage, indicators, and toys. Many more applications could be possible by tuning the range of trap depths used for energy storage. Very shallow traps could be used for temperature monitoring in, for example, cryopreservation. Deeper traps are useful for x-ray imaging and dosimetry. Next to these applications, a critical evaluation is made of the possibilities of persistent phosphors for applications such as solar energy storage and photocatalysis.



## I. INTRODUCTION

Persistent luminescence is an intriguing phenomenon that has fascinated people for a long time. It is defined as the long afterglow, sometimes erroneously called phosphorescence, present after the excitation of a luminescent material has stopped. Persistent luminescent materials are commonly called glow-in-the-dark phosphors, though not all materials giving off light for a long time without external excitation can be classified as persistent phosphors. Indeed, many living organisms such as glow worms, fireflies, sea sparkle (*Noctiluca scintillans*), some deep-sea fish, and fungi emit light, based on a (bio)chemical reaction, a phenomenon called chemiluminescence or more precisely, in living organisms, bioluminescence. Similarly, it is a common misconception among laymen that radioactive compounds show glow-in-the-dark persistent luminescence. Any picture of the water basin of an open nuclear reactor, showing a violet-blue glow, could lead to this conclusion, while this Cherenkov radiation is the direct result from charged particles, traveling faster than the phase velocity of light through the water. Also, up until the 1960s, radioactive elements were often combined with a ZnS-based phosphor, whereby the radiation was used to continuously excite the ZnS phosphor, effectively leading to persistent emission. Radium-226, an α-emitter with a half-lifetime of 1600 yr, was commonly used as the radioluminescence excitation source in watch dials and pushbuttons. Prometium-147, a β-emitter with a half-lifetime of 2.62 yr, was used in switch tips, radioluminescent panels, and lighting for the Apollo missions to the moon, thereby leading to some radiation hazards due to the radiation-induced degradation of the plastic cover of the radiation source.[1] Due to the safety risks associated with radioluminescent emitters and the emergence of much better "true" persistent luminescent emitters, using ionizing radiation for illumination purposes has become largely obsolete.

The present paper thus is only involved with the "true" persistent luminescent compounds. These consist of an inorganic host matrix doped with luminescent ions and, just like in non-persistent phosphors, the emission spectrum is determined by the combination of the intrinsic energy levels of the dopant ions and their interaction with the host lattice. When transition metal ions such as $Cr^{3+}$ or $Mn^{4+}$ are used, this electron–phonon and electron–ligand interaction is quite strong, and the dominant emission wavelength can be tuned to some extent.[2–4] Rare earth ions are by far the most popular dopants in phosphors; for most of them, the

emission stems from 4f–4f transitions that are well-shielded from the crystallographic environment and lead to sharp emission features with roughly constant wavelengths, independent of the host crystal into which they are incorporated. Notable exceptions are $Ce^{3+}$, $Yb^{2+}$, and $Eu^{2+}$, showing 5d–4f transitions in many hosts, which can be tuned over a broad wavelength range. Specifically, $Eu^{2+}$ is the "workhorse" of persistent phosphors,[5] and the best performing persistent luminescent materials known to date are $Eu^{2+}$-based: $SrAl_2O_4$:Eu,Dy, developed by Matsuzawa in 1994[6,7] and ubiquitous as a green emitter in emergency lighting, safety signs, and toys, $CaAl_2O_4$:Eu,Nd as a violet-blue emitter, and $Sr_2MgSi_2O_7$:Eu,Dy as a blue persistent phosphor. High performance red-emitting persistent phosphors are more scarce, not in the least because the eye sensitivity shifts to shorter wavelengths at low illumination levels, making the eyes less sensitive to red light.[8–10] As an illustration, Fig. 1 shows the normalized phosphor output during and after illumination with a blue LED, for the "normal" phosphor YAG:Ce ($Y_3Al_5O_{12}:Ce^{3+}$), having a very fast response and decay, and the benchmark persistent phosphor $SrAl_2O_4$:Eu,Dy.

In all cases—and this is the essential difference between an "ordinary" phosphor with a decay time in the range of nanoseconds to milliseconds and a persistent phosphor—the phenomenon of persistent luminescence relies on the existence of metastable trap levels that can temporarily store the excitation energy. In some cases, these trap levels are due to native defects, such as oxygen vacancies, but often, co-dopants like $Nd^{3+}$ or $Dy^{3+}$ in the above-mentioned cases, are used to introduce these trap levels.

Most persistent phosphors can be excited using x-rays (radioluminescence or RL), electrons (cathodoluminescence or CL), or UV/visible light (photoluminescence or PL). In all these cases, the persistent phosphor is showing "ordinary" luminescence with a short decay time, but at the same time, charge carriers are transferred from the activator to the traps and the traps are gradually filled. If the phosphor is illuminated for a sufficiently long time, a dynamic equilibrium of trap filling by the illumination and emptying traps by thermal excitation and optically stimulated luminescence (OSL) sets in.[12,13] If the excitation is stopped after this charging phase, the traps are slowly emptied by the thermal energy, available at room temperature, and energy can be transferred back to the dopant ions. This leads to strongly delayed luminescence, with a decay time up to hours, depending on the depth of the traps and the ambient temperature.

Up until the seminal work of Matsuzawa mentioned above, research activities on persistent phosphors were negligible for a long time, but after 1996, this field of research has strongly expanded, with currently over 250 publications per year (see Fig. 2). In the course of the years, several review papers, book chapters, and entire books have been published on persistent luminescence,[14–22] sometimes covering the entire field, sometimes focused on a specific class of materials like $Eu^{2+}$[5] or $Cr^{3+}$ and $Mn^{2+}$[23] doped persistent phosphors. In recent years, also a number of reviews have appeared, focused on a specific application, like near-infrared (NIR) bio-imaging.[16–19,24,25]

The present paper does not have the ambition to repeat any of these works which provide an excellent overview of persistent luminescence. Rather than looking back at all the prior achievements, this paper will look forward to possible future applications and challenges lying ahead to achieve these. An important section of the paper will also be devoted to ways of evaluating the performance of persistent phosphors. While some compounds may be performing poorly at room temperature, they may be excellently suited for applications at very low temperatures, where they can play a role in cryo-preservation or at higher temperatures like in bio-imaging. Ultimately, some traps are not emptied at room temperature for months, making them useful for personal dosimetry, or for thousands of years, rendering them into excellent materials

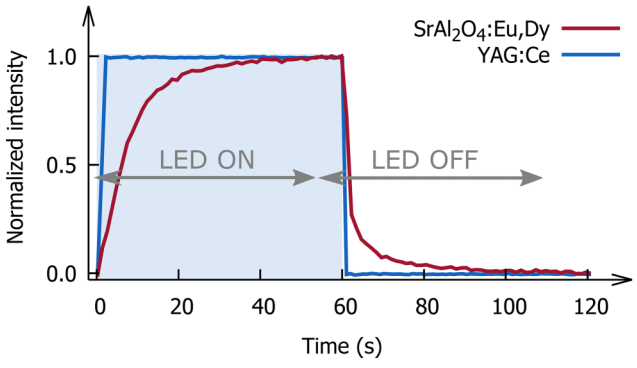


**FIG. 1.** Normalized emission from a "normal" phosphor YAG:Ce ($Y_3Al_5O_{12}:Ce^{3+}$) and the persistent phosphor $SrAl_2O_4$:Eu,Dy during and after excitation with a blue LED. Adapter with permission from Van der Heggen *et al.*, ACS Photonics **5**(11), 4529–4537 (2018). Copyright 2018 American Chemical Society.

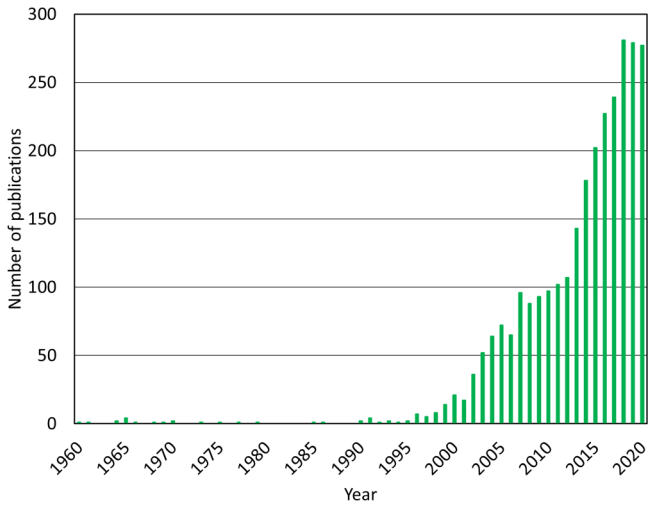


**FIG. 2.** Number of publications on persistent luminescence in the Web of Science (all databases); search string: **TS =** ("persistent luminescen*") *OR* **TS =** ("long afterglow") *OR* **TS =** ("long-lasting phosphorescen*") *OR* **TS =** ("persistent phosphor*") (accessed Nov 12, 2020).

for geological dating. While the latter compounds should normally not be classified as persistent phosphors, the only difference with "normal" persistent phosphors is the trap depth. Therefore, if a luminescent material contains metastable trap levels, a suitable application can typically be selected based on the depth of the traps, and a disadvantage for one application can become an advantage for a different application. Paraphrasing the famous quote assigned to Dutch former soccer player Johan Cruyff, "Every disadvantage has its advantage."

In the next paragraphs, we will first discuss the most common methods for the synthesis of persistent phosphors, each with its advantages and disadvantages. Then, the characteristics of persistent phosphors will be described, and the most suitable ways to evaluate their properties. After a brief overview of the different classes of suitable materials, the current and possible future applications will be presented, also adding a critical note to some unrealistic proposals. Finally, the possible improvements in performance lying ahead, and challenges to be tackled, will be discussed.

## II. SYNTHESIS METHODS FOR PERSISTENT PHOSPHORS

Since persistent phosphors are essentially, apart from the need for additional trap states, identical to other non-persistent phosphors, the same preparation methods are typically used. The most used and also the most straightforward method is high temperature solid state synthesis or "shake and bake." The biggest advantage of the method is its simplicity and the ease with which synthesis conditions can be changed. Most often, solid precursors containing the cations and anions needed for the final compound, are intimately ground and mixed in stoichiometric ratios in order to maximize the contact between the precursor particles. Once placed in a suitable crucible (often alumina), the mixed precursors are heated in a tube or muffle furnace up to a temperature, sufficient to induce a solid state reaction between the precursors, but below the melting temperature of the final compound. From a temperature around 200–300 °C below this melting temperature, there is a strong increase in the grain size of the final compound, a process called sintering.[26] Sintering typically leads to very a dense and strongly agglomerated material, which is not directly applicable as a phosphor. Therefore, post-synthesis grinding—manually or using a ball mill—is required in that case. Since many phosphor hosts are very hard materials, like oxides, nitrides, and oxynitrides, this particle size reduction is far from obvious and it is a definite advantage to keep the synthesis temperature to a point below the sintering temperature. Therefore, it is a delicate exercise for most materials to choose the right thermal processing conditions, allowing sufficient reaction and crystallization on the one hand, but preventing excessive sintering on the other hand. Ideally, the end product of the synthesis consists of well-crystallized micrometer-sized particles which, if partly agglomerated, can easily be separated using mild grinding.

Since the required temperatures can nevertheless be very high, up to about 1700 °C for some nitrides, fluxes are often used. Ideally, these are compounds that melt in between the precursor particles and promote easier interdiffusion, possibly also allow to dissolve the precursors, but do not take part in the reaction themselves. Popular flux materials are chlorides and fluorides,[27] but their use and optimization is more an art than science at the current stage of research. Some cases are known where the flux is partly incorporated into the final material, changing the phosphor's persistent luminescence characteristics.[28,29] In the case of $SrAl_2O_4$:$Eu^{2+}$(,$Dy^{3+}$), boric acid is a commonly added flux material. Adding boron to $SrAl_2O_4$:$Eu^{2+}$ generates mainly deeper traps, potentially related to new F-centers stabilized by the presence of (incorporated) boron.[30]

In some cases, it can be an advantage that sintering occurs. Given suitable conditions for densifying the phosphor to an almost pore-free ceramic, a highly efficient phosphor can be obtained.[31] In that case, the high efficiency is achieved because in a scatter-free sample, a large volume of material can be excited (or charged) and also contribute to the overall emission intensity. This approach should not be confused with the synthesis of phosphor-in-glass (PiG), whereby microscopic phosphor particles (photoluminescent particles or persistent luminescent particles) are incorporated in a glassy matrix.[32–35] The melt-quench technique used to prepare such composite materials was also named the frozen sorbet method.[36] A third and final approach for obtaining scatter-free phosphors is the direct incorporation of luminescent ions in an inorganic glass.[37]

Another parameter, apart from heating time and temperature, for the synthesis of persistent phosphors, is the atmosphere during heating. In the case of nitrides, nitrogen is an obvious choice. For sulfides, which was the most important class of phosphor materials for a long time,[38] synthesis in $H_2S$ is typically needed, immediately imposing stringent safety measures. In the case of oxides, air can usually be applied. However, while annealing in air is normally fine for the synthesis of an oxide host, some dopants, notably europium, can be oxidized, leading to the formation of fully oxidized $Eu^{3+}$ dopants. If $Eu^{2+}$ is the preferred valence state of this dopant, then it can be necessary to perform an additional thermal treatment in a reducing atmosphere.[39,40] In the latter case, it is a delicate exercise to sufficiently reduce the dopant without creating too much oxygen deficiency in the host, which can lead to grayish body colors of phosphors.[39] Concluding, it is very difficult to provide exact guidelines how to perform the solid state synthesis of a persistent phosphor. Usually, some trial and error is involved, choosing appropriate heating rates, heating times and temperatures, possible regrinding and reheating and a suitable gas atmosphere. In addition, when the procedure involves the synthesis of a persistent phosphor instead of an ordinary phosphor, the processing conditions can also influence the number of traps and trap characteristics, which are often not related to any dopant, but are attributed to intrinsic defects such as oxygen vacancies. Despite these complications, solid state reaction is still the most popular synthesis method and can yield materials with excellent performance.

Solid state reaction is the benchmark method for the synthesis of long afterglow compounds with optimum performance, but many applications—notably bio-imaging—require particles which are in the nanometer range rather than the micrometer range. For this purpose, solid state reaction is not applicable, unless there is a good way to decrease the size of the particles to the nanometer level. In this so-called top-down approach, particle size is reduced using planetary ball milling or laser ablation.

Ball milling is a purely mechanical method whereby particles are reduced in size by mechanical impact and friction. Typically,

powders are placed in a grinding jar, together with a number of hard grinding balls (often $Al_2O_3$ or $ZrO_2$) and a solvent so that a slurry is obtained. The grinding jar is then swung around in some kind of planetary motion in order to achieve maximum friction. Similar to the case of manual grinding using a mortar and pestle, the effect of the process is highly dependent on the size and hardness of the starting material. While it is effective in many cases, it also leads to a wide range of different particle sizes and, in order to obtain monodisperse particles, some kind of size selection has to be made. In addition, in most cases, the strong milling is detrimental to the afterglow properties of the persistent phosphor. There are a number of parameters that can influence the effects of milling: high energy/rotation speed vs low energy and the use of dry milling vs wet milling in a solvent, but in all cases, it is hard to avoid amorphization of the host and oxidation of the dopants due to surface exposure.[41–43] A post-milling thermal "healing" treatment, below the temperature where particle growth and sintering occurs, can then relax some of the undesired side effects of milling.

Laser ablation can be applied in two ways. If used in vacuum, it can be used as a thin film deposition technique (PLD or pulsed laser deposition), which has successfully led to persistent phosphors.[44,45] If the pulsed laser is used to ablate particles or targets in a liquid (a method commonly abbreviated as PLAL[46]), the ablated nanoparticles remain in suspension and can directly be used as nanophosphors.[47,48] In both variations of laser ablation, a phosphor powder is first made using the solid state reaction and subsequently converted to nanoparticles or thin films. While this kind of top-down approach to the synthesis of nanoparticles is successful in a number of cases, it is more obvious to opt for a bottom-up synthesis method, starting from liquid precursors.

Given the difficulties in controlling particle size, morphology and dispersion of phosphors prepared by the solid state reaction, a lot of research has been devoted to bottom-up synthesis methods. A major advantage of all these methods is the intimate mixing of the precursors, including dopants and co-dopants, on a molecular level, while in the solid state reaction, precursors have to react by solid diffusion. Another main advantage, and the main driving force for the research, is the possibility to control the particle size of the final products, by changing synthetic conditions such as pH, reaction temperature and time, precursor concentrations, etc. Sol-gel synthesis, colloidal synthesis, and co-precipitation all can lead to nanometer-range particles with excellent morphology and size distribution. Unfortunately, in many cases, it is necessary to perform a post-deposition thermal treatment to promote additional crystallization and improve the afterglow properties, thereby partly eliminating the advantages of a low temperature process with a well-defined particle morphology. Nevertheless, specific methods have been developed to allow this thermal annealing, while avoiding grain growth, for example, by temporarily or permanently embedding them in a silica matrix as a template.[49] High temperatures can be avoided if the liquid precursors are used in a solvothermal or hydrothermal process or are used in a microwave-assisted synthesis. The latter method—microwave assisted synthesis—can be applied in different ways. On the one hand, it is a way to speed up nucleation and crystal growth, starting from liquid precursors. It then can lead to nanometer-scale particles in a short synthesis time.[50] On the other hand, microwave-assisted solid state synthesis (MASS) has also gained some popularity as an alternative for the solid state synthesis in a tube or muffle furnace. Then, a microwave susceptor like graphite, surrounding the solid precursors, is needed to absorb the microwave energy, since these solid precursors typically show only minimal microwave absorption. Results are roughly equivalent to those obtained by the solid state synthesis, but the synthesis procedure can significantly be sped up.[40,51,52] The ultimate way to control the morphology and size of particles is templated growth, where a textured substrate or 3D porous structure is used to control particle properties.[53,54] Finally, combustion synthesis is a very fast but sometimes hard-to-control synthesis method. It has been very successful for a quite large range of phosphor compositions but can typically not compete with solid state synthesis in terms of optical performance.[55–60] For a more exhaustive treatment of the possible synthesis methods for persistent phosphors, we refer to some review papers[15,61] and the original research work. As a general conclusion, solid state reaction is still, despite its drawbacks, the best method for persistent phosphors with optimum afterglow performance. For applications requiring monodisperse or nanometer-range particles, chemical methods starting from liquid precursors are better suited. However, it still remains a challenge and a delicate balance to synthesize particles which are sufficiently small but at the same time show sufficient persistent luminescence. Ultimately, the amount of light that can be emitted from a particle is limited by the trapping capacity, i.e., the number of trap levels available for energy storage. Since the volume of a particle scales with the 3rd power of the diameter, smaller particles are clearly at a disadvantage in this respect. Nevertheless, in some nanoparticle systems, it has been reported that the afterglow intensity increases with decreasing particle size hinting at the involvement of surface defects in the trapping process.[62]

## III. MATERIALS FOR PERSISTENT LUMINESCENCE

After the publication on $SrAl_2O_4$:Eu,Dy as a highly efficient persistent, many research groups have started—or renewed—research on persistent luminescence. Due to the high performance of this specific phosphor, many phosphors emerging from this research were variations on a theme, changing cations, dopants, or co-dopants, in order to achieve equally good results, possibly in other wavelength ranges. Since the main application of persistent phosphors in the years after 1996 was in emergency and safety lighting, efforts were focused on visible light emitting materials. Both $CaAl_2O_4$:Eu,Nd and $Sr_2MgSi_2O_7$:Eu,Dy are excellent examples of such phosphors. Not surprisingly, $Eu^{2+}$ is the dopant of choice in these compounds: due to its electronic structure when incorporated in a crystalline matrix, $Eu^{2+}$ can be efficiently excited in the visible range and emission can be tuned over the entire visible spectrum, as seen in the overview of Fig. 3. In many phosphors, traps can be filled (at room temperature) via excitation to the lowest 5d level of $Eu^{2+}$. The same kind of trap filling through excitation to the lowest 5d level can be achieved in several $Ce^{3+}$ doped compounds, although in other $Ce^{3+}$ doped compounds an energy barrier needs to be overcome before trapping can occur.[63–65] While $Eu^{2+}$ was the dopant of choice for quite a number of years,[5] persistent phosphors using other dopants have been developed[66] as also

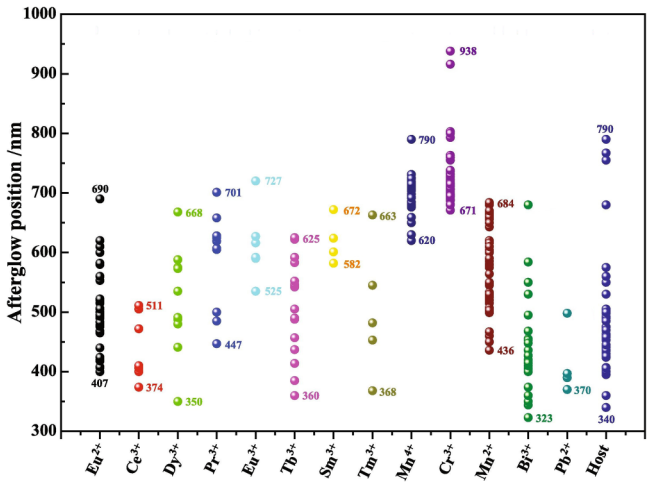


**FIG. 3.** Overview of common persistent phosphors, showing the combination of dopant and peak emission wavelength. Adapter with permission from Kang *et al.*, Chem. Eng. J. **403**, 126099 (2021). Copyright 2021 Elsevier.

shown in Fig. 3. Rare earth elements have mostly been used for visible light emission, and $ns^2$-ions ($Pb^{2+}$ and $Bi^{3+}$) have also had some attention, but mostly for UV emission.[67,68]

In most persistent phosphors, co-dopants are intentionally added to create trap levels or increase their number. The way to do this is currently still more art than science, since many aspects play a role. On the one hand, the efficiency of a phosphor is compromised by the presence of traps[11] and thus trap or defect density should be kept as low as possible. On the other hand, the very effect of persistent luminescence relies on the presence of a large number of traps, of the same order of magnitude as the number of dopants. Quite a number of persistent phosphors are known to be self-activated,[69] without the presence of co-dopants or even dopants.[70] This indicates that intrinsic defects, such as vacancies and lattice defects, can generate a sufficient number of luminescent and trap levels. However, in most cases, researchers try to harness the effect by choosing specific dopants and co-dopants for emission and trapping respectively, possibly aided by charge-compensating elements. Ideally, there should be some design rules or at least guidelines for the choice of the co-dopants in order to achieve appropriate dopant to co-dopant energy transfer (trapping) and subsequent de-trapping. As de-trapping is thermally activated, it is strongly dependent on the trap depth, i.e., the energy needed to release a charge carrier from its trap, leading to recombination and emission of a photon. Starting at around 2000,[71] Dorenbos published a series of papers building a semi-empirical model to predict the energy levels of rare earth ions in a host. This so-called Dorenbos model indeed provides guidelines on the depth of traps, as for instance adding $Sm^{3+}$ or $Tm^{3+}$ will lead to deeper electron traps compared to $Nd^{3+}$ and $Dy^{3+}$. It also allowed to design phosphors based on hole trapping.[72] On the other hand, the process of persistent luminescence is very sensitive on the exact trap depth, as a difference of 0.1 eV will already have a strong impact on the afterglow profile, challenging the accuracy of the empiric models.[73] An additional complication in many persistent phosphors is the interplay with other, native defects, obscuring the contribution of the lanthanide co-dopant itself or leading to contribution from the same lanthanide-based trap, but in different chemical environments. The consequence is that many persistent phosphors feature relatively broad trap depth distributions. This is in contrast to some other energy storage phosphors, like $YPO_4$:Ce,Ln, where well defined glow peaks are found.[74]

Initiated by the seminal work of Le Masne de Chermont *et al.* in 2007,[75] which presented a proof-of-concept for bio-imaging using a deep red/near-infrared (NIR) persistent phosphor, a lot of research has been devoted to the development of NIR persistent phosphors. For bio-imaging, emission in one of the so-called biological transparency windows is needed. The first such window spans the wavelength range from about 650 to 950 nm.[76] Using $Eu^{2+}$, an emission wavelength of 650 nm can easily be achieved for bio-imaging[46] and recently broad band IR emitting phosphors based on $Eu^{2+}$[77] and $Eu^{2+}/Tb^{3+}$[78] have been developed with emissions centered at around 740 and 810 nm, respectively. Nevertheless, other dopants are better suited for this application. $Mn^{2+}$ (showing broad band emission up to about 700 nm)[23] and $Mn^{4+}$ (with more narrowband emission at around 700 nm)[4,51,79,80] have both been explored, usually showing only limited afterglow performance. The best dopant for NIR persistent phosphors to date is $Cr^{3+}$. This dopant has been used in very efficient and long afterglow compounds and has been very successful in, among others, $ZnGa_2O_4$[81] and $LiGa_5O_8$.[82,83] In most cases, $Cr^{3+}$ shows sharp emission features at around 700 nm, but in compounds with a lower dopant-lattice crystal field interaction, also broad band emission has been reported,[84–86] up to well over 1000 nm.[87]

## IV. CHARACTERISTICS OF PERSISTENT PHOSPHORS

### A. Excitation characteristics

While persistent phosphors are often charged with UV or visible light with energies lower than the bandgap energy of the host, charging can also occur upon exposure to ionizing radiation such as x-rays or β radiation. However, examples can be found in the literature where different traps are filled upon exposure to ionizing radiation compared to optical excitation.[88,89] This is not surprising as optical charging often takes place through the direct excitation of the activator, while the ionizing radiation creates an avalanche of delocalized electron–hole pairs.

To evaluate the chargeable wavelength range for persistent luminescence, the persistent luminescence excitation spectrum or trap filling spectrum is usually used.[90] Often, photoluminescent emission in persistent phosphors can be effectively excited upon low energy light (e.g., red light for near-IR persistent phosphors); however, the majority cannot be charged for persistent luminescence, and only higher energy photons allow effective charging of the traps. A notable example is $LiGa_5O_8:Cr^{3+}$, which shows the typical three broad excitation bands in the UV, the blue and the red for photoluminescence, while only the UV band can efficiently charge the traps, leading to persistent luminescence.[82] It has been shown that the efficient NIR persistent phosphor $ZnGa_2O_4$:Cr can be charged using orange light, but then, charging occurs with a much lower efficiency than with UV excitation.[91]

### B. Emission characteristics

In the early stages, persistent phosphor research mainly focused on phosphors exhibiting emission in the visible region because the envisioned applications originally required the afterglow to be visible to the human eye. Figure 3 shows that emission over the entire visible range can be achieved. While numerous papers have been published on persistent phosphors using different dopants,[66] the best performing persistent phosphors in the visible are still $Eu^{2+}$ based. Thanks to the high sensitivity of its energy levels to the environment, changing the host can help tuning the $Eu^{2+}$ emission from violet to deep red.[5]

Over the past few years, new applications of persistent phosphors, such as sterilization of objects, anti-counterfeiting, or bio-imaging have been proposed. These applications require the development of persistent phosphors with emission in the UV[67,92,93] or the NIR (near infrared) to suit the requirements of these niche applications. As $Eu^{2+}$ emission cannot simply be tuned into the UV, these persistent phosphors use other dopants, like $Pr^{3+}$, $Pb^{2+}$, $Bi^{3+}$, or $Ce^{3+}$. Given the huge application potential of NIR emitting persistent phosphors in medical bio-imaging, many NIR-emitters have been developed, with $Cr^{3+}$[81–83] and—to a lesser extent—$Mn^{2+}$[23] and $Mn^{4+}$[4,51,94] as possible dopants.

### C. Trap properties: Trap depth and application potential

The temperature dependent persistent luminescence of a phosphor is largely determined by its corresponding trap depth(s) and the possible distribution of trap depths. Widespread utilization of persistent phosphors at various conditions relies on the dependence of persistent luminescence performance on the environmental temperature. The concept of the optimum working temperature, $T_{optimum}$, has been proposed as a criterion for the evaluation of a persistent phosphor. $T_{optimum}$ represents the temperature range at which the maximum afterglow output is achieved within a reasonable time frame.[95,96] This temperature can be related to the temperature of the main glow peak(s) of a thermoluminescence measurement and appears at a temperature about 20 to 30 °C below this glow peak temperature.[95,96] For example, CaS:Eu,Dy, which is known as a red-emitting persistent phosphor, has its highest integrated afterglow output at about −20 °C and, therefore, this phosphor is more suited for low temperature operations. On the other hand, $SrAl_2O_4$:Eu,Dy confirms its role as the best possible persistent phosphor for many applications, with an optimum working temperature around room temperature. The relation between the thermoluminescence glow curve and the optimum working temperature range is illustrated in Fig. 4 for a number of common persistent phosphors.

In the case of very shallow traps, these are emptied very fast at room temperature, and the optimum working temperature is, therefore, well below room temperature.[97] Very deep traps are never emptied at room temperature and only give rise to persistent luminescence at elevated temperatures. For a perspective on designing a persistent phosphor aiming at a certain temperature range, the energy levels of trap occupation should have specific depth accordingly to achieve efficient persistent luminescence for a certain ambient condition. The observation that many persistent phosphors

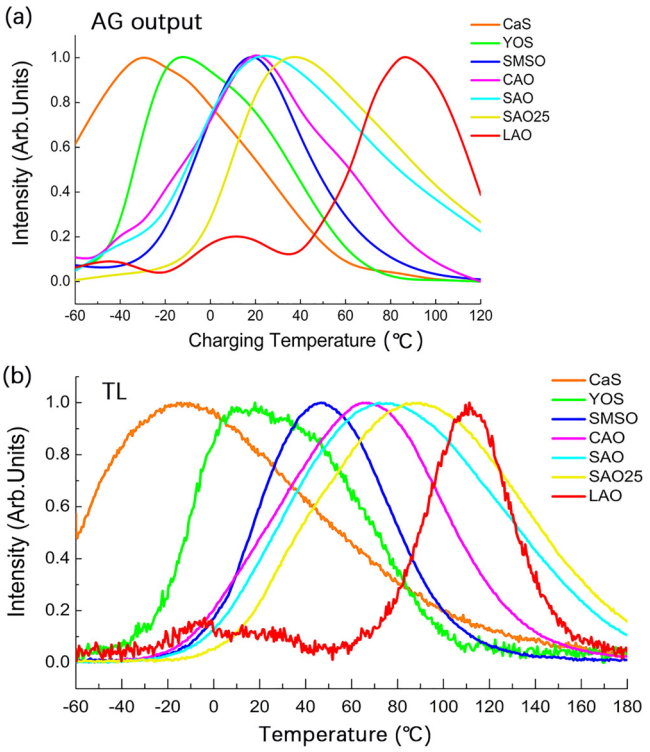


**FIG. 4.** Relation between the optimum working temperature range for maximum afterglow (a) and the thermoluminescence glow curve (b) for a number of common benchmark persistent phosphors. The legend for the different compounds can be found in the original publication. Adapter from Du *et al.*, Sci. Rep. **9**(1), 10517 (2019)., licensed under a Creative Commons Attribution 4.0 International License.

feature trap depth distributions, in contrast to a single, well-defined trap depth, points at different types of trapping defects. For most persistent phosphors, no detailed investigations have been undertaken to assign defects to specific trap depths and speculation often remains. Multiple explanations are possible, ranging from co-dopants being in slightly different chemical environments to different distances between trap and recombination center. For specific compounds, detailed spectroscopic and computational investigations were performed, like in the case of the antisite defect in $ZnGa_2O_4$:$Cr^{3+}$.[98,99] Using laser excitation and x-ray spectroscopy, it was it recently demonstrated that during trapping in $Sr_4Al_{14}O_{25}$:Eu,Dy, the dysprosium co-dopant acts as an electron trap, thereby forming $Dy^{2+}$.[100] Nevertheless, more research is needed to fully unravel all the defect structures relevant for the trapping.

### D. Trap properties: Number of traps and storage capacity

The performance of a persistent phosphor is usually evaluated by recording the time dependency of the afterglow intensity after excitation with a standard light source.[22] The units used to report these afterglow curves depend on the spectral characteristics of the

phosphor and the envisioned applications. The afterglow curves of phosphors emitting in the visible are usually expressed in photometric units, whereas NIR emitting phosphors, having an emission spectrum that falls outside of the spectral range of the eye sensitivity, are expressed in radiometric units. Nevertheless, a considerable fraction of the afterglow curves are reported in arbitrary units making a comparison between phosphors extremely difficult. Additionally, the morphology of the sample also plays an important role and it can, for example be expected that a transparent (glass-)ceramic sample will have an apparently better performance that a powder sample of the same size. For persistent phosphors emitting in the visible, the surface luminance should be specified in cd/m$^2$, thus allowing the comparison between different phosphor materials. The most information is then contained in an afterglow curve in absolute units, measured over a long time interval. Sometimes, an afterglow time is specified, vaguely mentioning "visible to the dark-adapted eye" or showing camera images after specified time intervals (without specifying camera settings). It is clear that such statements are scientifically of little value. As an illustration, Fig. 5 shows photographs of a commercial persistent luminescent emergency exit sign, imaged at different times after excitation and using different camera settings. Using these photographs, a "decay time" of well below 24 h or beyond 144 h (6 days) can both be "proven." Alternatively, a benchmark luminance of 0.32 mcd/m$^2$ (a value of 0.30 mcd/m$^2$ is also often used) is used to define the time until this value is reached as the afterglow lifetime. This luminance is not, as often erroneously stated, the ultimate eye sensitivity of the dark adapted eye, but about 100 times this limiting eye sensitivity. The absolute decay luminance of the same exit sign as pictured in Fig. 5 is shown in Fig. 6, together with the benchmark luminance, attained after 27.5 h.

Unfortunately, these photometric units do not allow to correctly compare the apparent brightness of persistent phosphors with a totally different emission spectrum. This is partly due to the Purkinje effect, which is the shift of the human eye sensitivity to shorter wavelengths at lower light intensities but also due to the gradual dark adaptation of the eyes. This shift from photopic (in light conditions) to scotopic vision (in dark conditions) is a highly complex photochemical process, which does not allow to

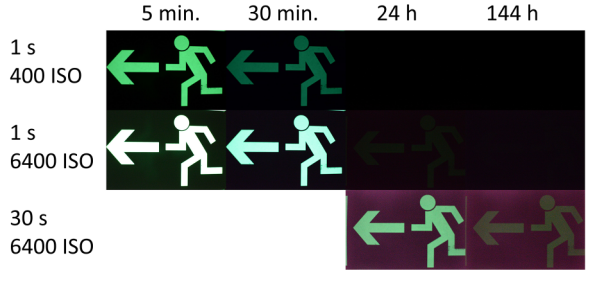


**FIG. 5.** Photographs of a commercial glow-in-the-dark emergency exit sign, taken at different times after excitation and using different camera settings. A Nikon D3200 digital camera was used with a 35 mm, f1.8 objective, and JPG image files were used without any post-processing. The sign was charged using a blacklight lamp at 365 nm during 10 min.

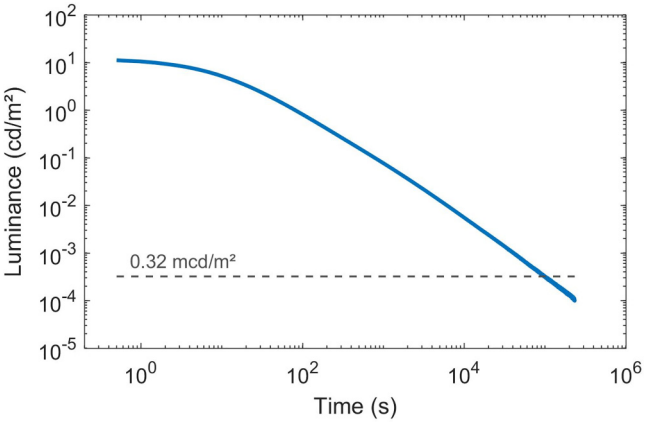


**FIG. 6.** Decay curve of the afterglow intensity of same exit sign as pictured in Fig. 5. The benchmark luminance of 0.32 mcd/m$^2$ is reached after 27.5 h.

describe the visual appearance of a light source under all possible conditions. Improvements in the description are, however, possible in some simple limiting cases and have led to concepts such as the unified luminance[101] and a visibility index.[8,9,22]

In the case of UV or NIR emitting phosphors, where the luminance in cd/m$^2$ is zero by definition, it is highly recommended to use the radiometric equivalent of the photometric luminance cd/m$^2$, which is mW/m$^2$/sr, as an absolute unit allowing comparison between different materials.[21] If K is the luminous efficacy of the radiation (LER) or photopic spectral luminous efficacy (PSLE), then K is a measure of the average eye sensitivity for this spectrum. For a pure green emitter at 555 nm, K would be (by definition of the candela) 683 lm/W, for a broadband green emitter like $SrAl_2O_4$:Eu,Dy, K is about 450 lm/W. Given that 1 cd =1 lm/sr, the benchmark luminance of 0.3 mcd/m$^2$, used to specify the lifetime of the persistent luminescence, can be converted to radiometric units as 0.3 mcd/m$^2$ = 0.3/K mW/m$^2$/sr. For a visible emitter with an average LER of K = 300 lm/W, the radiometric benchmark value would thus be $1 \times 10^{-3}$ mW/m$^2$/sr.[102] This value, and $5 \times 10^{-4}$ mW/m$^2$/sr,[79] has been used as a measure for the lifetime of a NIR emitting persistent phosphor, again allowing a direct comparison with other research work and other materials. It is definitely recommended that this modus operandi is getting more widespread use in UV or NIR persistent phosphor research.

A complementary alternative to quantify a phosphor's performance is to measure the storage capacity, which is expressed as a number of photons emitted by one gram of phosphor during the phosphor's afterglow. This metric allows to compare persistent phosphors, independent of their spectral characteristics and morphology. The storage capacity of the benchmark $SrAl_2O_4$:Eu,Dy phosphor has been found to amount to $(1.57 \pm 0.03) \times 10^{17}$ photons/gram which is equal to about 1.6% of the Eu activators being ionized, indicating that there is still a considerable margin for improvement, especially considering the fact that the storage capacity of other phosphors can be several orders of magnitude lower.[12]

A measurement of this storage capacity is fairly straightforward and only involves a few steps as explained in Van der Heggen *et al.*[12] First of all, phosphor needs to be incorporated into a transparent polymer, ensuring that all phosphor particles inside the layer can be uniformly excited and avoiding high phosphor loadings which could lead to shadowing effects. Next, the phosphor should be excited until saturation or dynamic equilibrium is reached. Preferably, this excitation takes place under conditions which are similar to the illumination conditions of the envisioned application. Next, the afterglow curve of the phosphor-containing polymer layer is recorded using a calibrated radiometric or photometric detector. Taking into account the angular dependency of the polymer layer's emission, the phosphor mass inside the layer and some unit specific conversion factors such as the luminous efficacy of the radiation or the average photon energy, this afterglow curve can be integrated over time to obtain the storage capacity of one gram of phosphor. The storage capacity obtained in this manner gives an indication of the phosphor's performance, independent of the spectral characteristics, the morphology or the equipment used to record the afterglow. If desired, the method can be extended to include optical or thermal stimulation in order to include deeper traps.

Finally, the phosphor performance also depends on the type of excitation source used. For instance, many persistent phosphors are easily chargeable in the UV, while excitation at longer wavelengths is often not efficient to fill traps, due to the presence of (thermal) energy barriers for the trapping process. Hence, it is important to always specify in detail the type, spectral output, and intensity of the excitation source. Preferably, those parameters are chosen to mimic the intended application. For instance, excitation with orange or red light is more sensible than using UV radiation in the case of *in vivo* bioimaging applications.[91]

## V. PRESENT AND FUTURE APPLICATIONS

### A. Safety signage and toys

Persistent phosphors are perhaps best known for their use in a variety of objects such as toys, watches, and wall decorations. They are only incorporated into these objects to provide them with a glow-in-the-dark feature and as such they are not essential to the workings of these applications. However, in other applications, persistent phosphors are indispensable for a flawless operation and consequently these applications impose more stringent requirements with respect to initial brightness and duration of the phosphor's afterglow. An example of a successfully commercialized application that fully relies on the afterglow of persistent phosphors is the glow-in-the-dark safety signage in buildings and airplanes. In this case, the use of a persistent phosphor ensures that the safety signage remains visible, even in the case of a power outage.

In addition to the widespread use of persistent phosphors in toys and safety signage, many new applications are being proposed every year. The list of possible applications includes the use persistent phosphors in glow-in-the-dark road markings, for bioimaging, for photocatalysis, to reduce flickering in AC-driven LEDs, as pressure sensors[103,104] or to visualize ultrasound beams.[105,106] However, not all these proposed applications are equally feasible and the limited performance of the current generation of persistent phosphors hampers their use in most of these challenging applications. In what follows, we will discuss some of the applications mentioned above and elaborate on the challenges that need to be faced to enable their wide-spread implementation. Figure 7 provides a graphical overview of the current, future, and hard-to-achieve applications. Details on these different applications can be found further in the text.

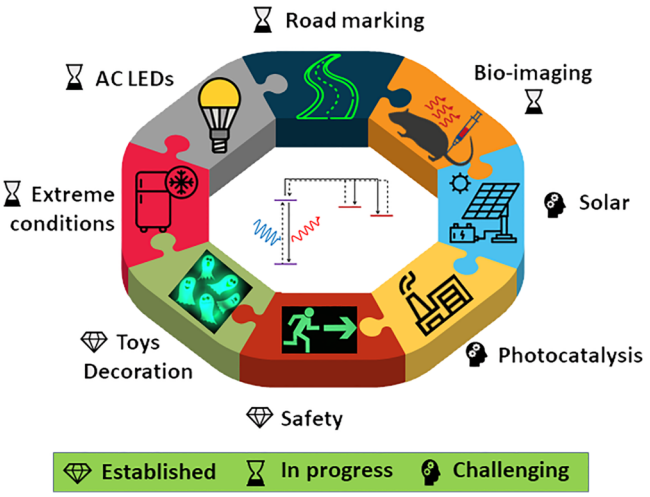


**FIG. 7.** Overview of reported or potential applications of persistent phosphors. Details on the different applications are found in the text. The different qualifications (established, in progress or challenging) of the different applications are based on the personal assessment by the authors. This figure has been designed using resources from Flaticon.com.

### B. Road markings

The idea to use persistent phosphors in glow-in-the-dark road markings has been proposed a few years ago as a way to avoid the use of street lighting without any loss of visibility of the road markings.[107,108] This application bears a close resemblance to the use of persistent phosphors in safety signage, but it suffers from drawbacks that are inherently related to the use of persistent phosphors under outdoor conditions. The most important difference between in- and outdoor conditions is the lack of a controlled temperature. While the underlying broad trap depth distribution allows to use most commercially available persistent phosphors over a very broad temperature range, the difference in temperature between charging of the phosphor (during the day) and emission of the afterglow (during the night) can lead to a notable reduction of the afterglow intensity.[108] Although the best persistent phosphors are fit for common safety applications, where emergency signage should typically remain visible for one hour after power stoppage, the storage capacity does not yet allow to bridge a full night, hampering the application in road markings. In contrast, similar application areas have been proposed, such as glow-in-the-dark bicycle paths, where the light emission is not absolutely vital, but offers additional guidance.

### C. Flicker reduction in AC-LEDs

Notwithstanding the obvious similarities between persistent phosphors and phosphors for solid state lighting or display applications, these two fields in luminescence research rarely overlap. An exception can be found in the use of persistent phosphors in AC-driven LEDs. It has recently been proposed that the extended luminescence lifetime of the afterglow can be used to bridge the dark periods during which the LEDs are not emitting, thereby reducing the temporal variations in the overall intensity of the LEDs.[109–116] In contrast to some of the benchmark phosphors with afterglow times of several hours, the persistent phosphors used in AC-driven LEDs should have afterglow times of the order of a few tens of milliseconds in order to reduce the flicker due to the pulsation of the LEDs, at double the main frequency (50–60 Hz). While the idea of using persistent phosphors in AC-LEDs seems to have gained popularity over the past few years, the recently reported loss in quantum efficiency due to optically stimulated luminescence by excitation light has raised some concerns about their applicability in solid state lighting. At the very least, it has shown that the absorption characteristics of the filled traps should be taken into account when designing new persistent phosphors.[11] In addition, the trap depth distribution should be designed to match the elevated temperature of the LED chip during operation. Finally, the storage capacity should be matched with the LED intensity, to avoid saturation of the persistent luminescence in high brightness LEDs.

### D. NIR bio-imaging

Persistent luminescence imaging has been regarded as the next generation of autofluorescence-free long-term optical bio-imaging technology. A proof-of-concept[75] work published in 2007 realized the application of *in vivo* imaging by using the near-infrared persistent luminescent material $Ca_{0.2}Zn_{0.9}Mg_{0.9}Si_2O_6:Eu^{2+}$, $Dy^{3+}$, $Mn^{2+}$ as a biomarker, hereby opening up new avenues for the widespread uses of persistent luminescent phosphors. Other pioneering work published in 2014 proposed a novel low-energy red photons chargeable *in vivo* imaging method by using chromium-doped zinc gallate as a near-infrared emitting persistent luminescent label in the NIR-I region (650–950 nm), to track labeled cells *in vivo*. As for the use of *in vivo* imaging, the emitting wavelength of the phosphor is required to be located in the biological optical window (i.e., the first near-infrared window in the wavelength between 650 nm and 950 nm or the second near-infrared window in the wavelength between 1000 nm and 1350 nm). In these wavelength ranges, scattering, absorption, and autofluorescence are limited, and biological tissue is partly transparent. Thus, the development of deep-red or near-infrared emitting persistent phosphors has attracted much attention for application to *in vivo* bio-imaging systems or medical imaging. Both optical windows are illustrated in Fig. 8, together with the attenuation coefficients of some tissue components, and the response curves of typical detectors.

Near-infrared-emitting persistent nanophosphors, as potential candidates for *in vivo* bio-imaging applications, are ideally expected to be operating at 37 °C (normothermia, as the normal human body temperature). Currently, $Cr^{3+}$-doped near-infrared emitting persistent luminescence phosphors are used as the key component

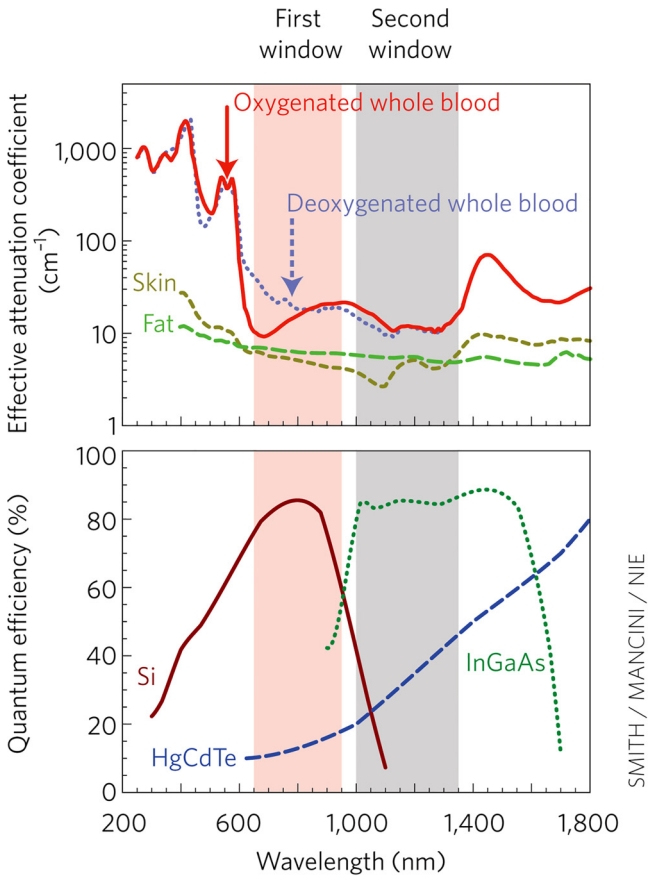


**FIG. 8.** Illustration of the optical windows that can be used for optical bio-imaging, in the shaded areas. The top figure shows the effective attenuation coefficient of a number of tissue components (including absorption and scattering); the bottom figure shows the quantum efficiencies of typical detectors for this wavelength range. Reproduced with permission from Smith *et al.*, Nat. Nanotechnol. **4**(11), 710–711 (2009). Copyright 2009 Springer Nature Limited.

for *in vivo* imaging in small animals, such as $ZnGa_2O_4:Cr^{3+}$,[81,91] $MgGa_2O_4:Cr^{3+}$,[117,118] $Zn_3Ga_2Ge_2O_{10}:Cr^{3+}$, $Zn_3Ga_2SnO_8:Cr^{3+}$, and $LiGa_5O_8:Cr^{3+}$.[82,83] For some types of phosphors, like $LaAlO_3:Mn^{4+}$, which is also a NIR-emitting persistent phosphor proposed for bio-imaging, the ideal working temperature is at 90 °C,[95] and it turns out to be hard to lower the trap depth in order to achieve efficient afterglow at 37 °C. Alternatively, many $Mn^{4+}$-doped phosphors also provide near-infrared persistent emission.[4,51,79,94] However, compared to the $Cr^{3+}$-doped representatives, the near-infrared persistent luminescence from $Mn^{4+}$ doped phosphors is still largely restricted due to the large amount of deeper traps which do not contribute significantly to the afterglow at room temperature or normothermia. In summary, it remains a challenge to fine-tune the trap depths to increase the near-infrared afterglow performance around the normal human body temperature. Further in-depth investigations on the so-called trap engineering are still needed by either a traditional trial-and-error approach or a design way

through combining band structure engineering and crystal synthesis optimization. Currently, the emission from the rare earth ions $Nd^{3+}$ and $Er^{3+}$ is being explored for bio-imaging in the second optical window (for $Nd^{3+}$, at around 1064 nm and 1340 nm[119–121]) and a third optical window above 1500 nm (using $Er^{3+}$ emission[122]). The low absorption strength of the 4f–4f transitions of these ions can be overcome through excitation and energy transfer from ions like $Cr^{3+}$ and $Ce^{3+}$, both having a much larger absorption cross section than the rare earth ions.[122,123]

### E. Persistent phosphors at extreme conditions

For the most common applications, persistent phosphors should have their optimum working conditions—a good compromise between initial luminance and decay time—at room temperature. If the depth of the traps is lower, then the traps are emptied even below room temperature, and the decay time of the persistent phosphor is very short. However, there are specific niche applications where phosphors with such shallow traps can perfectly applied, for example, in cryo-preservation.[97] If this kind of phosphor is charged at very low temperature, e.g., liquid nitrogen temperature, then the traps remain filled for a very long time, and no light is emitted. If the temperature increases, then traps are emptied. Therefore, connecting a persistent phosphor with shallow traps to a sample which should remain at liquid nitrogen temperature for preservation (like a biological sample or virus) allows to check if the cold chain of the sample was broken, even after a very long time of storage.

Some compounds have very deep traps that remain filled for weeks or months at room temperature. These are ideally suited as so-called TLDs (thermoluminescence dosimeters) and are extensively used for personal dosimetry badges or for medical imaging plates.[124] If the traps are even deeper, then energy can be stored in them for periods of thousands of years, and radiation-induced defects in common minerals like quartz and felspars can be used successfully for geological dating.[125] While the only big difference between these compounds and "normal" persistent phosphors is the trap depth, both types of materials can hardly be considered persistent phosphors, fall far outside the scope of this paper and will not be considered further.

### F. Nighttime solar energy

It is generally accepted that phosphors can play a role in increasing the efficiency of solar cells. When a phosphor is positioned on top of a solar cell, it can convert short wavelength photons to longer wavelength photons (down-shifting) for which the solar cell is more efficient or, using a down-converting phosphor, one high energy incoming photon can be converted to two photons. If an upconversion phosphor is positioned below the solar cell, it can be used to absorb low energy photons that are transmitted through the cell and convert them to higher energy photons which can contribute to the photocurrent.[126] Persistent phosphors can equally be used as down-shifting phosphors for this application.

Next, authors have tried to use a persistent phosphor to act as an illumination source for a solar cell during the night. Unfortunately, it is a simple calculation to estimate the "sunlight equivalent" energy that can be stored in a persistent phosphor of a given thickness, and this amounts to only a few seconds of sunlight at best. Therefore, given the state of the art in persistent phosphors, this application should be regarded as inefficient. Furthermore, even with one order of magnitude higher storage capacity, the sunlight equivalent will still be marginal. Some reported performances of solar cells using a persistent phosphor during the night were a nighttime solar cell efficiency of 0.0076%,[127] or a generated power density of 56 $\mu$W/cm$^2$,[128] values which might be sufficient to keep low power electronic devices running, but are unable to boost the overall efficiency of a solar power plant. Finally, potential losses during daytime because of the presence of the persistent phosphor (e.g., scattering, escape cone and non-radiative losses) could easily outweigh the nighttime gains.

### G. Photocatalysis

Over the last decade, there has been an increasing interest for using long persistent phosphors in photocatalysis applications. Here, typically, a long persistent phosphor is combined with a photocatalyst, where, if illumination has stopped, the former activates the latter, resulting in prolonged photocatalysis. The most used photocatalyst nowadays is the anatase phase of $TiO_2$, despite a lot of research investigating alternatives.[129–131]

Several researchers investigated different long persistent phosphors combined with $TiO_2$. Locardi *et al.*[132] supported $TiO_2$ nanoparticles on $(3ZnO{:}Ga_2O_3{:}2GeO_2){:}1\%Cr^{3+}$ persistent luminescent material to degrade methylene blue (MB) in an aqueous solution. In the absence of external illumination, photodegradation of MB was observed. Vaiano *et al.*[133] coupled commercial $Sr_{2.90}Eu_{0.03}Dy_{0.07}Al_4SiO_{11}$ with N-doped $TiO_2$ for the photocatalytic degradation of crystal violet dye in solution. By this coupling, the researchers were able to obtain an energy saving of 42% for the 90% removal of crystal violet by alternating the state of the light source (ON/OFF). Feng *et al.*[134] investigated the decomposition of MB by using $CdSiO_3{:}Gd^{3+},Bi^{3+}$ coated with $TiO_2$ nanoparticles. The long persistent luminescent $CdSiO_3{:}Gd_{3+},Bi_{3+}$ was able to increase the photocatalytic activity of $TiO_2$ in dark conditions, i.e., without UV illumination. Moreover, it increased the overall photocatalytic activity under illumination with UV light.

Other photocatalysts than $TiO_2$ were investigated for this application. For example, a $g\text{-}C_3N_4$@Au composite as a photocatalyst, combined with $SrAl_2O_4{:}Eu^{2+},Dy^{3+}$ as a long persistent phosphor.[135] The addition of Au to $g\text{-}C_3N_4$ enhances visible light absorbance of this composite. Degradation tests of Rhodamine B (RhB) and photocatalytic hydrogen evolution from water showed that the $g\text{-}C_3N_4$@Au@$SrAl_2O_4{:}Eu^{2+},Dy^{3+}$ composite maintained some photocatalytic activity in dark conditions after irradiation for 10 min.

This typical combination of a long persistent phosphor and a photocatalytic material is not the only method to obtain this effect. Feng *et al.*[136] proposed, instead of combining long persistent luminescence and photocatalysis, a new concept called "long persistent photocatalysis," where a material is synthesized that can, after illumination, store electrons in the traps, but avoids the recombination of the released electrons and holes. This can be avoided by reducing the particle size. By synthesizing $MgGa_2O_4$ nanorods, they were

able to achieve decomposition of RhB in solution even when irradiation was stopped.

It is still not certain what is the underlying mechanism of the combination of long persistent luminescence with photocatalysis. On the one hand, when irradiation has stopped, the long persistent luminescence can act as a light source for the photocatalyst;[69] however, this light output is known to be very weak in intensity, especially compared to the external light source (typically mercury or xenon discharge lamps or high power UV LEDs). On the other hand, if a close contact is obtained between the long persistent phosphor and the photocatalyst, charge transfer processes can occur, where the charges (holes and electrons) transfer to the photocatalyst surface, inducing photocatalysis without the emission of photons by the long persistent phosphor.[137] It is also a possibility that these two mechanisms operate simultaneously. Finally, experiments to separate all the possible effects, including blank measurements without photocatalyst, dark measurements, effective surface area measurements, effects of phosphor diffusion and degradation, are all essential to fully understand the involved processes, but are not always conducted in detail. Further research is clearly required in order to get a better understanding in this principle and to improve the efficiency of this phenomenon. Nevertheless, the synergy between persistent phosphors and photocatalysts, how improbable it may sound, seems to work, which is a sufficient reason to invest some efforts in its further investigation.

## VI. CONCLUSIONS

It is clear that we have come a long way since the ZnS-based glow-in-the dark watch dials, excited using radioactive compounds. Thanks to a number of breakthroughs and the efforts of many, persistent luminescence is now a mature technology, with a large variety of compounds, allowing a large number of applications. Especially in the field of emergency lighting, persistent phosphors are highly successful.

Next to these successes, there are still many pieces of the puzzle missing and improvements need to be made. In a number of cases, the interactions between dopants and co-dopants have been identified,[100] but in many cases, synthesis of a persistent phosphor with specific properties is still more art than science. One important parameter, the trap depth and its distribution, is hard to control, and leads to persistent phosphors with totally different working temperatures. While this can be seen as a disadvantage, it can also be used in favor of niche applications such as cryo-preservation or personal dosimetry. Another important parameter is the number of traps that can be filled, the so-called trapping capacity.[12] Even for the most performant persistent phosphor, it turns out that the number of filled traps is less than 2% of the number of activators. For specific phosphors, this is attributed to the high efficiency of OSL (optically stimulated luminescence), whereby the traps are emptied due to the excitation light that is used to charge the persistent phosphor.[11,13] This seems like a fundamental limiting factor and it is a challenge to find ways to charge persistent phosphors while avoiding OSL during this charging phase, or to find phosphors not showing any efficient OSL, which would require the investigation of other co-dopants or methods to introduce optically non-active defects.

With the current state of the art, some applications are only marginally possible, like glow-in-the-dark road markings. This is partly due to the limited storage capacity of persistent phosphors, but also due to the inherent temperature dependence of the phenomenon. As long as the detrapping phenomenon is thermally driven, this seems hard to avoid, a dopant–trap interaction which is based on tunneling and which would be largely independent of temperature, would make a world of a difference in this respect.

## DATA AVAILABILITY

The data that support the findings of this study are available from the corresponding author upon reasonable request.

## REFERENCES

[1]R. A. English, R. E. Benson, J. V. Bailey, and C. M. Barnes, *NASA Technical Note* (NASA, Washington DC, 1973),Vol. TN D-7080.
[2]Z. Jia, C. Yuan, R. Li, P. Sun, R. Dong, Y. Liu, L. Wang, H. Jiang, and J. Jiang, Phys. Chem. Chem. Phys. **22**(18), 10343–10350 (2020).
[3]S. Q. Liu, Z. Z. Wang, H. Cai, Z. Song, and Q. L. Liu, Inorg. Chem. Front. **7**(6), 1467–1473 (2020).
[4]J. R. Du and D. Poelman, Ceram. Int. **45**(7), 8345–8353 (2019).
[5]K. Van den Eeckhout, P. F. Smet, and D. Poelman, Materials **3**(4), 2536–2566 (2010).
[6]T. Matsuzawa, Y. Aoki, N. Takeuchi, and Y. Murayama, J. Electrochem. Soc. **143**(8), 2670–2673 (1996).
[7]Y. Murayama, N. Takeuchi, Y. Aoki, and T. Matsuzawa, Patent No. US5424006A (June 13, 1995).
[8]D. Poelman, N. Avci, and P. F. Smet, Opt. Express **17**(1), 358–364 (2009).
[9]D. Poelman and P. F. Smet, Opt. Express **18**(25), 26293–26299 (2010).
[10]D. Poelman and P. F. Smet, Opt. Express **19**(20), 18808–18809 (2011).
[11]D. Van der Heggen, J. J. Joos, and P. F. Smet, ACS Photonics **5**(11), 4529–4537 (2018).
[12]D. Van der Heggen, J. J. Joos, D. C. Rodriguez Burbano, J. A. Capobianco, and P. F. Smet, Materials **10**(8), 867 (2017).
[13]C. Tydtgat, K. W. Meert, D. Poelman, and P. F. Smet, Opt. Mater. Express **6**(3), 844–858 (2016).
[14]R. E. Rojas-Hernandez, F. Rubio-Marcos, M. Á. Rodriguez, and J. F. Fernandez, Renew. Sust. Energy Rev. **81**, 2759–2770 (2018).
[15]Y. Li, M. Gecevicius, and J. Qiu, Chem. Soc. Rev. **45**(8), 2090–2136 (2016).
[16]L. Liang, N. Chen, Y. Y. Jia, Q. Q. Ma, J. Wang, Q. Yuan, and W. H. Tan, Nano Res. **12**(6), 1279–1292 (2019).
[17]J. Liu, T. Lecuyer, J. Seguin, N. Mignet, D. Scherman, B. Viana, and C. Richard, Adv. Drug Delivery Rev. **138**, 193–210 (2019).
[18]H. Tan, T. Wang, Y. Shao, C. Yu, and L. Hu, Front. Chem. **7**, 387 (2019).
[19]S. Q. Wu, Y. Li, W. H. Ding, L. T. Xu, Y. Ma, and L. B. Zhang, Nano-Micro Lett. **12**(1), 70 (2020).
[20]S. Wu, Z. Pan, R. Chen, and X. Liu, *Long Afterglow Phosphorescent Materials* (Springer, Cham, Switzerland, 2017).
[21]J. Xu and S. Tanabe, J. Lumin. **205**, 581–620 (2019).
[22]P. F. Smet, K. Van den Eeckhout, O. Q. De Clercq, and D. Poelman, in *Handbook on the Physics and Chemistry of Rare Earths*, edited by J.-C. Bünzli and V. K. Pecharsky (Elsevier, 2015), Vol. 48, pp. 1–108.
[23]Y. X. Zhuang, Y. Katayama, J. Ueda, and S. Tanabe, Opt. Mater. **36**(11), 1907–1912 (2014).
[24]Q. S. Lin, Z. H. Li, and Q. Yuan, Chin. Chem. Lett. **30**(9), 1547–1556 (2019).
[25]P. L. Suarez, M. Garcia-Cortes, M. T. Fernandez-Arguelles, J. R. Encinar, M. Valledor, F. J. Ferrero, J. C. Campo, and J. M. Costa-Fernandez, Anal. Chim. Acta **1046**, 16–31 (2019).

[26]V. B. Kravchenko, Y. L. Kopylov, and V. A. Kotel'nikov, in *Handbook of Solid-State Lasers*, edited by B. Denker and E. Shklovsky (Woodhead Publishing, 2013), pp. 54–81.
[27]L. Liu, R. J. Xie, C. Zhang, and N. Hirosaki, Materials **6**(7), 2862–2872 (2013).
[28]A. Nag and T. R. N. Kutty, J. Alloys Compd. **354**(1-2), 221–231 (2003).
[29]A. Nag and T. R. N. Kutty, Mater. Res. Bull. **39**(3), 331–342 (2004).
[30]J. Bierwagen, T. Delgado, G. Jiranek, S. Yoon, N. Gartmann, B. Walfort, M. Polnau, and H. Hagemann, J. Lumin. **222**, 117113 (2020).
[31]J. Xu, J. Ueda, K. Kuroishi, and S. Tanabe, Scr. Mater. **102**, 47–50 (2015).
[32]D. Q. Chen, W. D. Xiang, X. J. Liang, J. S. Zhong, H. Yu, M. Y. Ding, H. W. Lu, and Z. G. Ji, J. Eur. Ceram. Soc. **35**(3), 859–869 (2015).
[33]W. Li, Y. Zhuang, P. Zheng, T. L. Zhou, J. Xu, J. Ueda, S. Tanabe, L. Wang, and R. J. Xie, ACS Appl. Mater. Interfaces **10**(32), 27150–27159 (2018).
[34]E. A. Salazar-Valenzuela, J. Alvarado-Rivera, C. Chapa, and M. E. Alvarez-Ramos, Phys. Status Solidi A **217**(17), 2000226 (2020).
[35]R. Zhang, H. Lin, Y. L. Yu, D. Q. Chen, J. Xu, and Y. S. Wang, Laser Photonics Rev. **8**(1), 158–164 (2014).
[36]T. Nakanishi, Y. Katayama, J. Ueda, T. Honma, S. Tanabe, and T. Komatsu, J. Ceram. Soc. Jpn. **119**(1391), 609–615 (2011).
[37]K. Asami, J. Ueda, and S. Tanabe, J. Lumin. **207**, 246–250 (2019).
[38]P. F. Smet, I. Moreels, Z. Hens, and D. Poelman, Materials **3**(4), 2834–2883 (2010).
[39]N. Avci, K. Korthout, M. A. Newton, P. F. Smet, and D. Poelman, Opt. Mater. Express **2**(3), 321–330 (2012).
[40]J. Miranda de Carvalho, D. Van der Heggen, L. I. D. J. Martin, and P. F. Smet, Dalton Trans. **49**(14), 4518–4527 (2020).
[41]R. E. Rojas-Hernandez, F. Rubio-Marcos, E. Enriquez, M. A. De La Rubia, and J. F. Fernandez, RSC Adv. **5**(53), 42559–42567 (2015).
[42]S. K. Kandpal, B. Goundie, J. Wright, R. A. Pollock, M. D. Mason, and R. W. Meulenberg, ACS Appl. Mater. Interfaces **3**(9), 3482–3486 (2011).
[43]V. Havasi, D. Tatrai, G. Szabo, E. Varga, A. Erdohelyi, G. Sipos, Z. Konya, and A. Kukovecz, J. Lumin. **219**, 116917 (2020).
[44]K. Sato, S. Komuro, T. Morikawa, H. Aizawa, T. Katsumata, S. Harako, and X. Zhao, J. Cryst. Growth **275**(1-2), E1137–E1141 (2005).
[45]P. D. Nsimama, O. M. Ntwaeaborwa, and H. C. Swart, J. Lumin. **131**(1), 119–125 (2011).
[46]T. Maldiney, G. Sraiki, B. Viana, D. Gourier, C. Richard, D. Scherman, M. Bessodes, K. Van den Eeckhout, D. Poelman, and P. F. Smet, Opt. Mater. Express **2**(3), 261–268 (2012).
[47]S. K. Singh, K. Kumar, and S. B. Rai, Mater. Sci. Eng. B **166**(2), 180–184 (2010).
[48]G. Ledoux, D. Amans, C. Dujardin, and K. Masenelli-Varlot, Nanotechnology **20**(44), 445605 (2009).
[49]E. Glais, M. Pellerin, V. Castaing, D. Alloyeau, N. Touati, B. Viana, and C. Chaneac, RSC Adv. **8**(73), 41767–41774 (2018).
[50]S. G. Menon, A. K. Kunti, S. D. Kulkarni, R. Kumar, M. Jain, D. Poelman, J. J. Joos, and H. C. Swart, J. Lumin. **226**, 117482 (2020).
[51]J. Du and D. Poelman, Nanomaterials **9**(12), 1759 (2019).
[52]C. C. S. Pedroso, J. M. Carvalho, L. C. Rodrigues, J. Holsa, and H. F. Brito, ACS Appl. Mater. Interfaces **8**(30), 19593–19604 (2016).
[53]P. F. Smet and D. Poelman, J. Phys. D Appl. Phys. **42**(9), 095306 (2009).
[54]X. H. Tan, J. Alloys Compd. **477**(1–2), 648–651 (2009).
[55]N. J. Zuniga-Rivera, R. Garcia, R. Rodriguez-Mijangos, V. Chemov, R. Melendrez, M. Pedroza-Montero, and M. Barboza-Flores, Nucl. Instrum. Methods Phys. Res. Sect. B **326**, 99–102 (2014).
[56]C. L. Zhao, D. H. Chen, Y. H. Yuan, and M. Wu, Mater. Sci. Eng. B Solid State Mater. Adv. Technol. **133**(1-3), 200–204 (2006).
[57]R. Ruiz-Torres, V. Chernov, P. Salas-Castillo, N. J. Zuniga-Rivera, L. A. Diaz-Torres, R. Melendrez, and M. Barboza-Flores, Opt. Mater. **101**, 109763 (2020).
[58]Z. Qiu, Y. Zhou, M. Lü, A. Zhang, and Q. Ma, Acta Mater. **55**(8), 2615–2620 (2007).
[59]J. Kim, C. K. Lee, and Y. J. Kim, Opt. Mater. **104**, 109944 (2020).
[60]T. Gotoh, M. Jeem, L. H. Zhang, N. Okinaka, and S. Watanabe, J. Phys. Chem. Solids **142**, 109436 (2020).
[61]Z. H. Zhou, Y. Y. Li, and M. Y. Peng, Chem. Eng. J. **399**, 125688 (2020).
[62]G. A. Mandl, D. Van der Heggen, D. R. Cooper, J. J. Joos, J. Seuntjens, P. F. Smet, and J. A. Capobianco, Nanoscale **12**, 20759–20766 (2020).
[63]J. Ueda, K. Kuroishi, and S. Tanabe, Proc. SPIE **8987**, 89870L (2014).
[64]J. Ueda, K. Kuroishi, and S. Tanabe, Appl. Phys. Lett. **104**(10), 101904 (2014).
[65]J. Ueda, J. Ceram. Soc. Jpn. **123**(1444), 1059–1064 (2015).
[66]K. Van den Eeckhout, D. Poelman, and P. Smet, Materials **6**(7), 2789–2818 (2013).
[67]P. Xiong and M. Peng, Opt. Mater. X **2**, 100022 (2019).
[68]T. Lyu and P. Dorenbos, Chem. Mater. **32**(3), 1192–1209 (2020).
[69]F. Kang, G. Sun, P. Boutinaud, H. Wu, F.-X. Ma, J. Lu, J. Gan, H. Bian, F. Gao, and S. Xiao, Chem. Eng. J. **403**, 126099 (2021).
[70]C. Agamah, S. Vuori, P. Colinet, I. Norrbo, J. M. de Carvalho, L. K. Okada Nakamura, J. Lindblom, L. van Goethem, A. Emmermann, T. Saarinen, T. Laihinen, E. Laakkonen, J. Lindén, J. Konu, H. Vrielinck, D. Van der Heggen, P. F. Smet, T. L. Bahers, and M. Lastusaari, Chem. Mater. **32**, 8895–8905 (2020).
[71]P. Dorenbos, J. Lumin. **91**(1-2), 91–106 (2000).
[72]T. Lyu and P. Dorenbos, J. Mater. Chem. C **6**(2), 369–379 (2018).
[73]J. J. Joos, D. Poelman, and P. F. Smet, Phys. Chem. Chem. Phys. **17**(29), 19058–19078 (2015).
[74]A. J. J. Bos, P. Dorenbos, A. Bessiere, A. Lecointre, M. Bedu, M. Bettinelli, and F. Piccinelli, Radiat. Meas. **46**(12), 1410–1416 (2011).
[75]Q. le Masne de Chermont, C. Chaneac, J. Seguin, F. Pelle, S. Maitrejean, J. P. Jolivet, D. Gourier, M. Bessodes, and D. Scherman, Proc. Natl. Acad. Sci. U.S.A. **104**(22), 9266–9271 (2007).
[76]A. M. Smith, M. C. Mancini, and S. Nie, Nat. Nanotechnol. **4**(11), 710–711 (2009).
[77]J. Qiao, G. Zhou, Y. Zhou, Q. Zhang, and Z. Xia, Nat. Commun. **10**(1), 5267 (2019).
[78]J. J. Joos, D. Van der Heggen, L. I. D. J. Martin, L. Amidani, P. F. Smet, Z. Barandiaran, and L. Seijo, Nat. Commun. **11**(1), 3647 (2020).
[79]J. Du, O. Q. De Clercq, K. Korthout, and D. Poelman, Materials **10**(12), 1422 (2017).
[80]Y. Li, Y.-Y. Li, K. Sharafudeen, G.-P. Dong, S.-F. Zhou, Z.-J. Ma, M.-Y. Peng, and J.-R. Qiu, J. Mater. Chem. C **2**(11), 2019–2027 (2014).
[81]A. Bessiere, S. Jacquart, K. Priolkar, A. Lecointre, B. Viana, and D. Gourier, Opt. Express **19**(11), 10131–10137 (2011).
[82]O. Q. De Clercq, L. I. D. J. Martin, K. Korthout, J. Kusakovskij, H. Vrielinck, and D. Poelman, J. Mater. Chem. C **5**(41), 10861–10868 (2017).
[83]F. Liu, W. Yan, Y. J. Chuang, Z. Zhen, J. Xie, and Z. Pan, Sci. Rep. **3**, 1554 (2013).
[84]V. Rajendran, M. H. Fang, G. N. De Guzman, T. Lesniewski, S. Mahlik, M. Grinberg, G. Leniec, S. M. Kaczmarek, Y. S. Lin, K. M. Lu, C. M. Lin, H. Chang, S. F. Hu, and R. S. Liu, ACS Energy Lett. **3**(11), 2679–2684 (2018).
[85]A. Zabiliute, S. Butkute, A. Zukauskas, P. Vitta, and A. Kareiva, Appl. Opt. **53**(5), 907–914 (2014).
[86]L. L. Zhang, S. Zhang, Z. D. Hao, X. Zhang, G. H. Pan, Y. S. Luo, H. J. Wu, and J. H. Zhang, J. Mater. Chem. C **6**(18), 4967–4976 (2018).
[87]G. N. A. De Guzman, M.-H. Fang, C.-H. Liang, Z. Bao, S.-F. Hu, and R.-S. Liu, J. Lumin. **219**, 116944 (2020).
[88]V. Boiko, J. Zeler, M. Markowska, Z. Dai, A. Gerus, P. Bolek, E. Zych, and D. Hreniak, J. Rare Earths **37**(11), 1200–1205 (2019).
[89]E. Chandrawanshi, D. P. Bisen, N. Brahme, G. Banjare, T. Richhariya, and Y. Patle, J. Mater. Sci. Mater. Electron. **31**(17), 14454–14465 (2020).
[90]A. J. J. Bos, R. M. van Duijvenvoorde, E. van der Kolk, W. Drozdowski, and P. Dorenbos, J. Lumin. **131**(7), 1465–1471 (2011).
[91]T. Maldiney, A. Bessiere, J. Seguin, E. Teston, S. K. Sharma, B. Viana, A. J. Bos, P. Dorenbos, M. Bessodes, D. Gourier, D. Scherman, and C. Richard, Nat. Mater. **13**(4), 418–426 (2014).

[92]Y. M. Yang, Z. Y. Li, J. Y. Zhang, Y. Lu, S. Q. Guo, Q. Zhao, X. Wang, Z. J. Yong, H. Li, J. P. Ma, Y. Kuroiwa, C. Moriyoshi, L. L. Hu, L. Y. Zhang, L. R. Zheng, and H. T. Sun, Light Sci. Appl. **7**(1), 88 (2018).
[93]X. Wang, Y. Chen, F. Liu, and Z. Pan, Nat. Commun. **11**(1), 2040 (2020).
[94]J. Du, O. Q. De Clercq, and D. Poelman, Ceram. Int. **44**(17), 21613–21620 (2018).
[95]J. Du, O. Q. De Clercq, and D. Poelman, Sci. Rep. **9**(1), 10517 (2019).
[96]J. Du, A. Feng, and D. Poelman, Laser Photonics Rev. **14**(8), 2070048 (2020).
[97]J. Du and D. Poelman, Adv. Opt. Mater. **8**(6), 1901848 (2020).
[98]A. De Vos, K. Lejaeghere, D. E. Vanpoucke, J. J. Joos, P. F. Smet, and K. Hemelsoet, Inorg. Chem. **55**(5), 2402–2412 (2016).
[99]D. Gourier, A. Bessiere, S. K. Sharma, L. Binet, B. Viana, N. Basavaraju, and K. R. Priolkar, J. Phys. Chem. Solids **75**(7), 826–837 (2014).
[100]J. J. Joos, K. Korthout, L. Amidani, P. Glatzel, D. Poelman, and P. F. Smet, Phys. Rev. Lett. **125**(3), 033001 (2020).
[101]M. S. Rea, J. D. Bullough, J. P. Freyssinier-Nova, and A. Bierman, Light. Res. Technol. **36**(2), 85–109 (2004).
[102]O. Q. De Clercq, J. Du, P. F. Smet, J. J. Joos, and D. Poelman, Phys. Chem. Chem. Phys. **20**(48), 30455–30465 (2018).
[103]A. Feng and P. F. Smet, Materials **11**(4), 484 (2018).
[104]R. R. Petit, S. E. Michels, A. Feng, and P. F. Smet, Light Sci. Appl. **8**(1), 124 (2019).
[105]M. Kersemans, P. F. Smet, N. Lammens, J. Degrieck, and W. Van Paepegem, Appl. Phys. Lett. **107**, 234102 (2015).
[106]T. Zhan, C.-N. Xu, O. Fukuda, H. Yamada, and C. Li, Ultrason. Sonochem. **18**(1), 436–439 (2011).
[107]J. Nance and T. D. Sparks, Prog. Org. Coat. **148**, 105749 (2020).
[108]J. Botterman and P. F. Smet, Opt. Express **23**(15), A868–A881 (2015).
[109]C. W. Yeh, Y. Li, J. Wang, and R. S. Liu, Opt. Express **20**(16), 18031–18043 (2012).
[110]J. Ueda, K. Kuroishi, and S. Tanabe, Appl. Phys. Express **7**(6), 062201 (2014).
[111]Y. F. Liu, P. Liu, L. Wang, C. E. Cui, H. C. Jiang, and J. Jiang, Chem. Commun. **53**(77), 10636–10639 (2017).
[112]H. Lin, J. Xu, Q. Huang, B. Wang, H. Chen, Z. Lin, and Y. Wang, ACS Appl. Mater. Interfaces **7**(39), 21835–21843 (2015).
[113]H. Lin, B. Wang, J. Xu, R. Zhang, H. Chen, Y. Yu, and Y. Wang, ACS Appl. Mater. Interfaces **6**(23), 21264–21269 (2014).
[114]H. Lin, B. Wang, Q. M. Huang, F. Huang, J. Xu, H. Chen, Z. B. Lin, J. M. Wang, T. Hu, and Y. S. Wang, J. Mater. Chem. C **4**(43), 10329–10338 (2016).
[115]B. W. Li, J. H. Zhang, M. Zhang, Y. B. Long, and X. He, J. Alloys Compd. **651**, 497–502 (2015).
[116]L. Chen, Y. Zhang, S. Xue, X. Deng, L. Anqi, F. Liu, Y. Jiang, S. Chen, and A. Bahader, Funct. Mater. Lett. **06**(04), 1350047 (2013).
[117]Y. Zhao, J. R. Du, X. W. Wu, Y. F. Wang, and D. Poelman, J. Lumin. **220**, 117035 (2020).
[118]N. Basavaraju, S. Sharma, A. Bessiere, B. Viana, D. Gourier, and K. R. Priolkar, J. Phys. D Appl. Phys. **46**(37), 375401 (2013).
[119]B. Nimmegeers, E. Cosaert, T. Carbonati, D. Meroni, and D. Poelman, Materials **13**(16), 3564 (2020).
[120]B. del Rosal, D. H. Ortgies, N. Fernández, F. Sanz-Rodríguez, D. Jaque, and E. M. Rodríguez, Adv. Mater. **28**(46), 10188–10193 (2016).
[121]I. Villa, A. Vedda, I. X. Cantarelli, M. Pedroni, F. Piccinelli, M. Bettinelli, A. Speghini, M. Quintanilla, F. Vetrone, U. Rocha, C. Jacinto, E. Carrasco, F. S. Rodríguez, Á Juarranz, B. del Rosal, D. H. Ortgies, P. H. Gonzalez, J. G. Solé, and D. J. García, Nano Res. **8**(2), 649–665 (2015).
[122]J. Xu, D. Murata, J. Ueda, and S. Tanabe, J. Mater. Chem. C **4**(47), 11096–11103 (2016).
[123]J. Xu, S. Tanabe, A. D. Sontakke, and J. Ueda, Appl. Phys. Lett. **107**(8), 081903 (2015).
[124]P. Leblans, D. Vandenbroucke, and P. Willems, Materials **4**(6), 1034–1086 (2011).
[125]L. Bøtter-Jensen and A. S. Murray, Radiat. Prot. Dosim. **84**(1), 307–315 (1999).
[126]B. M. van der Ende, L. Aarts, and A. Meijerink, Phys. Chem. Chem. Phys. **11**(47), 11081–11095 (2009).
[127]J. F. Zhang, J. M. Lin, J. H. Wu, S. Zhang, P. Zhou, X. Chen, and R. Xu, J. Mater. Sci.: Mater. Electron. **27**(2), 1350–1356 (2016).
[128]A. Puntambekar and V. Chakrapani, Phys. Rev. B **93**(24), 245301 (2016).
[129]A. Fujishima, X. T. Zhang, and D. A. Tryk, Surf. Sci. Rep. **63**(12), 515–582 (2008).
[130]M. Ni, M. K. H. Leung, D. Y. C. Leung, and K. Sumathy, Renew. Sust. Energy Rev. **11**(3), 401–425 (2007).
[131]M. Pelaez, N. T. Nolan, S. C. Pillai, M. K. Seery, P. Falaras, A. G. Kontos, P. S. M. Dunlop, J. W. J. Hamilton, J. A. Byrne, K. O'Shea, M. H. Entezari, and D. D. Dionysiou, Appl. Catal. B **125**, 331–349 (2012).
[132]F. Locardi, E. Sanguineti, M. Fasoli, M. Martini, G. A. Costa, M. Ferretti, and V. Caratto, Catal. Commun. **74**, 24–27 (2016).
[133]V. Vaiano, O. Sacco, and D. Sannino, J. Cleaner Prod. **210**, 1015–1021 (2019).
[134]P. Feng, Y. Wei, Y. Wang, J. Zhang, H. Li, and Z. Ci, J. Am. Ceram. Soc. **99**(7), 2368–2375 (2016).
[135]X. M. Liu, X. Y. Chen, Y. Z. Li, B. Q. Wu, X. B. Luo, S. Ouyang, S. L. Luo, A. A. Al Kheraif, and J. Lin, J. Mater. Chem. A **7**(32), 19173–19186 (2019).
[136]P. Feng, J. Zhao, J. Zhang, Y. Wei, Y. Wang, H. Li, and Y. Wang, J. Alloys Compd. **695**, 1884–1890 (2017).
[137]L. Li, K. Xu, Y. Wang, Z. Hu, and H. Zhao, Opt. Mater. Express **6**, 1122–1130 (2016).